DINAME 2023 - Proceedings of the XIX International Symposium on Dynamic Problems of Mechanics,
A.S. De Paula, A.T. Fabro and M.R. Machado (Editors), ABCM.
Pirenópolis, Go, Brazil, February 26th to March 3rd, 2023

Nonlinear dynamics of a magnetic shape memory alloy oscillator

Jean M. Souza [1], Luciana Loureiro S. Monteiro [1] and Marcelo A. Savi [2]

[1] Centro Federal de Educação Tecnológica Celso Suckow da Fonseca, CEFET/RJ - Department of Mechanical Engineering 20.271.110, Rio de Janeiro, Brazil

[2] Universidade Federal do Rio de Janeiro, COPPE - Department of Mechanical Engineering, Center for Nonlinear Mechanics 21.941.972, Rio de Janeiro, PO Box 68.503, Brazil

Abstract: Magnetic shape memory alloys (MSMAs) represent a class of smart materials that can exhibit large magnetic field induced strain when subjected to magneto-mechanical loadings. The induced strain can be achieved by martensitic variant reorientation or field induced phase transformation. The martensitic reorientation mechanism has the advantage to provide high frequency actuation, since it does not rely on phase transformation between strain cycles, which would demand cooling periods. This kind of behavior is not extensively explored in the literature, which is the objective of this work. In this regard, an MSMA single degree-of-freedom nonlinear oscillator is investigated, exploiting the system response under different conditions. A phenomenological model is employed to describe the MSMA behavior, proposing a dynamical system model. Numerical simulations are carried out using the fourth order Runge-Kutta method. Simulations show that the application of a bias magnetic field on a MSMA based dynamical system leads to changes in the oscillation period and the mean displacement of the system. Therefore, MSMAs have a potential use to provide adaptive dynamical behavior. Moreover, complex behaviors can be achieved, including chaos.

Keywords: Magnetic shape memory alloys, martensitic variant reorientation, nonlinear dynamics.

INTRODUCTION

Smart materials represent a special class of materials that presents multiphysics coupling which means that their properties can be modified by the application of an external stimuli, such as mechanical stress, heat, magnetic or electric fields. This remarkable characteristic enables them to be widely explored in industrial devices, as actuators, sensors, and energy harvesters. Magnetic shape memory alloys (MSMAs) are smart materials that exhibit a thermo-magneto-mechanical coupling. This kind of material can undergo a magnetic field induced strain (MFIS) of up to 10% when subjected to a magneto-mechanical loading (Smith et al., 2014). MFIS can be generated by two different mechanisms: magnetic field induced phase transformation; and martensitic variant reorientation. The magnetic field induced phase transformation requires a larger magnetic field, presenting a larger blocking stress when compared with the martensitic variant reorientation mechanism (Haldar et al., 2014). Among the MSMAs, the most widely explored using the reorientation phenomenon is the Ni-Mn-Ga alloy, due to its high magneto-crystalline anisotropic energy and low twinning stress.

The magnetic field induced strain on MSMAs was first reported in 1996 (Ullakko et al., 1996) and since then, many phenomenological models have been developed (Chen et al., 2014; O'Handley, 1998; Wang and Steinmann, 2012). Kiefer and Lagoudas (2005) and Kiefer (2007) developed a thermodynamical model introducing internal state variables to describe the variant reorientation phenomenon. Shirani and Kadkhodaei (2014a, 2014b) proposed improvements on this model allowing the phenomenon description for every stress level with a single set of parameters, and using a single phase diagram, regardless the magneto-mechanical loading. Souza et al. (2018) developed a new model for MSMA based on the generalized standard material approach.

Although the quasi-static loading has been treated in many works, the dynamical behavior of MSMA systems has not been widely explored. This work deals with a dynamical investigation of MSMA systems. The constitutive model proposed by Kiefer (2007) is employed, considering the improvements proposed by Shirani and Kadkhodaei (2014a, 2014b). A one-degree of freedom nonlinear oscillator is proposed, and numerical simulations are carried out using the fourth order Runge-Kutta method considering frequency sweep and magnetic field sweep. The effect of the application of a bias magnetic field is investigated.

Mathematical Model

The phenomenological description of MSMAs considers a bidimensional magneto-mechanical loading composed by axial stress and transversal bias magnetic field. Irreversible thermodynamics is employed to propose a consistent model that follows the Clausius-Duhem inequality. Two martensitic variants are assumed (1 is favored by the compressive stress, and 2 is favored by the transversal bias magnetic field), represented by the volume fraction variable. Upon mechanical loading, if the stress required to initiate the reorientation process is surpassed, the martensitic volume fraction begins to change, and the MSMA undergoes inelastic strain. Thus, the overall strain (ε) is treated by considering the sum of elastic

(ε^e) and inelastic strain (ε^r), due to the reorientation process. The inelastic strain is written as a function of the martensitic variant 2 volume fraction. Therefore, the constitutive equation is described by:

$$\varepsilon = \frac{\sigma}{E} + (1-\xi)\varepsilon^{r,max} \tag{1}$$

where the first term of the sum refers to the elastic and the second to the inelastic strain; $\varepsilon^{r,max}$ is the maximum reorientation strain that can be induced through the variant reorientation phenomena, ξ is the martensitic variant 2 volume fraction and σ is the stress; E stands for the elasticity modulus of the material, and since both martensitic variants have different modulus, it is written as follows:

$$E = \xi E_2 + (1-\xi)E_1 \tag{2}$$

where E_2 is the elasticity modulus of variant 2, and E_1 is the modulus for variant 1. The equations for the ξ evolution are written as a function of the applied stress and magnetic field, being derived from the Gibbs free energy function. For more details regarding the phenomenological model description see Kiefer (2007) and Shirani and Kadkhodaei (2014a). After the formulation of the constitutive equations, consider an MSMA dynamical system composed by a mass coupled to an MSMA element and a linear viscous damping, depicted in Fig. 1. An external force $F(t)$ is exciting the system, being composed by a sum of harmonic and steady force (due to a pre-stress). On this basis, the dimensionless equations of motion are presented in the sequel:

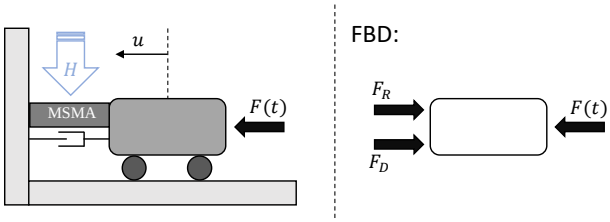

Figure 1 – Dynamic system and free body diagram

$$\begin{cases} x' = v \\ v' = \left(\frac{1}{mL\omega_0^2}\right)[F_C + F_0\sin(\Omega\tau)] - \left(\frac{\omega_n}{\omega_0}\right)^2 (x - \varepsilon^r) - \frac{c}{m\omega_0}v \end{cases} \tag{3}$$

where m is the lumped mass, c is the linear viscous coefficient and the MSMA element may be considered as a bar with length L and cross-sectional area A; ω_n is related to the natural frequency of the system, which can be written as $\omega_n = \sqrt{\frac{(EA/L)}{m}}$; ω_0 is a reference frequency defined as the equivalent natural frequency when the MSMA sample is composed by the martensitic variant 2: $\omega_0 = \sqrt{\frac{(E_2A/L)}{m}}$. In addition, Ω is the dimensionless frequency, defined as the ratio between the harmonic force frequency (ω) and ω_0: $\Omega = \frac{\omega}{\omega_0}$; $\tau = \omega_0 t$ is the dimensionless time; $x = \frac{u}{L}$ is the dimensionless displacement; v is the dimensionless velocity. F_C is a steady compressive force and F_0 is the amplitude of the harmonic force. The steady force represents a pre-stress applied to ensure that the material works under compression in order to allow reorientation process. An initial setpoint is adopted in order to assure that the system is working under compression.

Numerical Simulations

Numerical simulations are carried out considering an operator split approach where phenomenological and dynamical problems are solved separately, assuming a trial state where phase transformations do not occur. The trial state allows the determination of the predictor step where the displacement is calculated using the fourth order Runge-Kutta method and, afterward, used as the input strain loading on the phenomenological model. A corrector step is then performed defining, and an iterative process should be performed until variables converge through a tolerance. The system parameters for the simulations are taken from the dynamical model introduced in Chen and He (2020) (Tab. 1) together with phenomenological model parameters (Shirani and Kadkhodaei, 2014a). A pre-stress of 4.5 MPa is adopted together with a harmonic stress amplitude of 5 MPa. Different magnetic fields are treated: 0; 0.4; and 0.6 MA/m. The parameters $\sigma_{x0}^{s(2,1)}$ and $\sigma_{x0}^{f(2,1)}$ are critical stresses in which reverse reorientation starts and finishes in the absence of external magnetic fields, respectively. $\mu_0 H_{y0}^{f(1,2)}$ and $\mu_0 H_{y0}^{f(1,2)}$ are the magnetic fields in which forward reorientation starts and finishes and $\mu_0 H_y^{cr}$ is the critical magnetic field, above which both forward and reverse reorientation are not affected by the magnetic field. The parameter $\mu_0 H_y^l$ is the limiting magnetic field, below which the stresses for reverse reorientation are approximately constant, regardless the magnetic field.

Table 1 – Phenomenological model and system parameters

Properties	Values	Properties	Values	Properties	Values
$\sigma_{x0}^{s(2,1)}$	0.6 MPa	$\mu_0 H_y^l$	0.055 MA/m	m	0.0225 kg
$\sigma_{x0}^{f(2,1)}$	2 MPa	M^{sat}	0.625 MA/m	L	15 mm
$\mu_0 H_{y0}^{s(1,2)}$	0.140 MA/m	E_1	2.4 GPa	A	6 mm²
$\mu_0 H_{y0}^{f(1,2)}$	0.363 MA/m	E_2	0.4 GPa	c	10.1 kg/s
$\mu_0 H_y^{cr}$	0.6 MA/m	$\varepsilon^{r,max}$	0.058		

Figure 2 shows bifurcation diagrams representing the slow quasi-static variation of the forcing frequency for three levels of magnetic fields. It is noticeable that the increase of the magnetic field is related to more complex responses associated with cloud of points, Fig. 2 (b) and (c), while a period-1 response is the typical case without magnetic field, a case without reorientation. Under magnetic field, the system presents bifurcations from a period-1 to a period-2 response and then, to a period-4 just by increasing the excitation frequency. A chaotic-like behavior is identified in the region with a cloud of points.

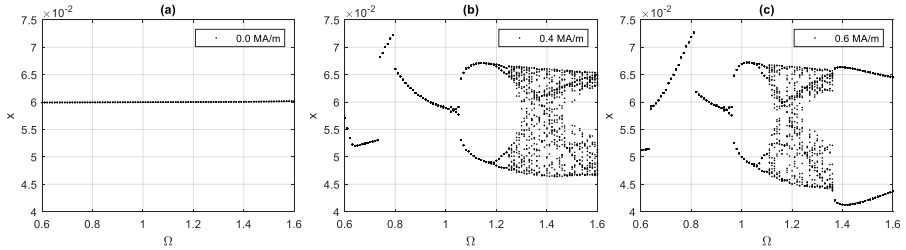

Figure 2 – Bifurcation diagram in respect with Ω for: (a) 0.0 MA/m; (b) 0.4 MA/m; (c) 0.6 MA/m

Figure 3 shows simulations when $\mu_0 H = 0.6$ MA/m and three excitation frequencies, presenting the phase-space, the time history of the volume fraction and the stress, and the stress-strain diagrams of the MSMA element. The stress-strain diagram and the volume fraction allow one to observe the martensitic reorientation processes during the dynamical response, which is close related to the complexity of the dynamical response. Note that the system presents a period-1 response when $\Omega = 0.9$, changing to a period-2 for $\Omega = 1.0$, and period-4 when $\Omega = 1.1$.

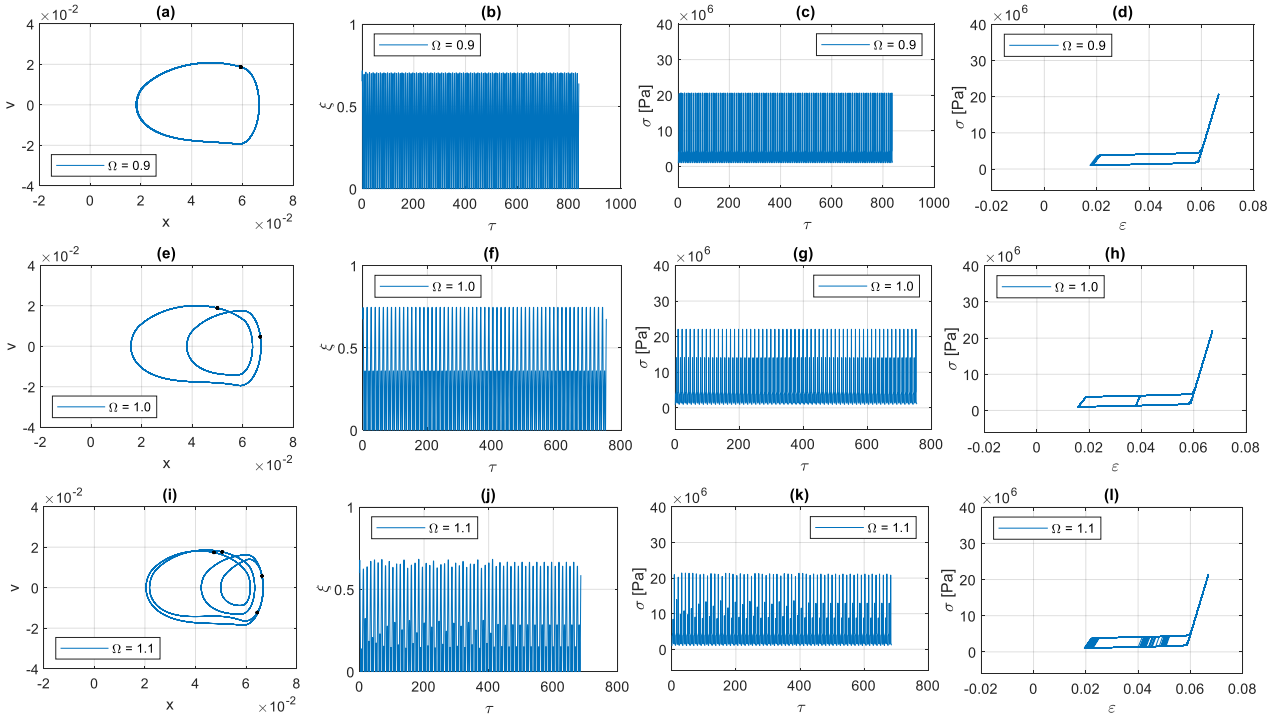

Figure 3 – $\mu_0 H = 0.6$ MA/m : phase-space (a, e, i); time history of the volume fraction (b, f, j); time history of the stress (c, g, k); and stress-strain diagram (d, h, l) for, respectively, $\Omega = 0.9$, $\Omega = 1.0$ and $\Omega = 1.1$.

The root-mean-square of the displacement is calculated as $x_{rms} = \sqrt{\frac{(\sum_{i=1}^{n} x_i^2)}{n}}$, and Figure 4 presents this variable showing its variation as the excitation frequency is slowly increased for three bias magnetic field levels. It is noticeable that, the bias magnetic field leads to lower mean displacements, and the case without bias magnetic field has not

reorientation, and the mean displacement of the system is kept constant around $x_{rms} = 0.06$, which means that MSMA has an elastic response. It should be pointed out that there is an abrupt drop in x_{rms} associated with the following frequencies: $\Omega = 0.63$ for 0.6 MA/m; and $\Omega = 0.73$ for 0.4 MA/m. Afterward, the x_{rms} value slowly increases as the excitation frequency is raised. Although, after the x_{rms} drop, the difference between the root-mean-square displacement for 0.4 MA/m and 0.6 MA/m seemed negligible from $\Omega = 0.74$ to $\Omega = 1.3$.

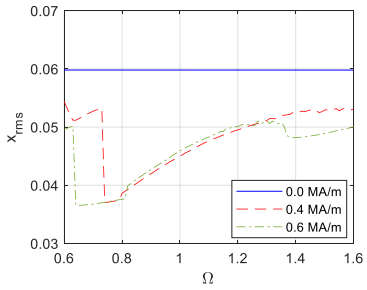

Figure 4 – Root-mean-square of the displacement.

This behavior is analyzed in more detail by considering the response close to these frequencies. For 0.4 MA/m, the main abrupt changes occurs between $\Omega = 0.73$ and $\Omega = 0.74$. Figure 5 depicts the phase-space, the time history of the volume fraction and the stress, and the stress-strain diagrams of the MSMA rod for these two frequencies. One can see that, when the frequency is slightly increased, the wider displacement induces a more severe cyclic variant reorientation: for $\Omega = 0.73$, the peak value for the volume fraction is approximately $\xi = 0.25$; for $\Omega = 0.74$, a complete reorientation occurs ($\xi_{max} = 1$).

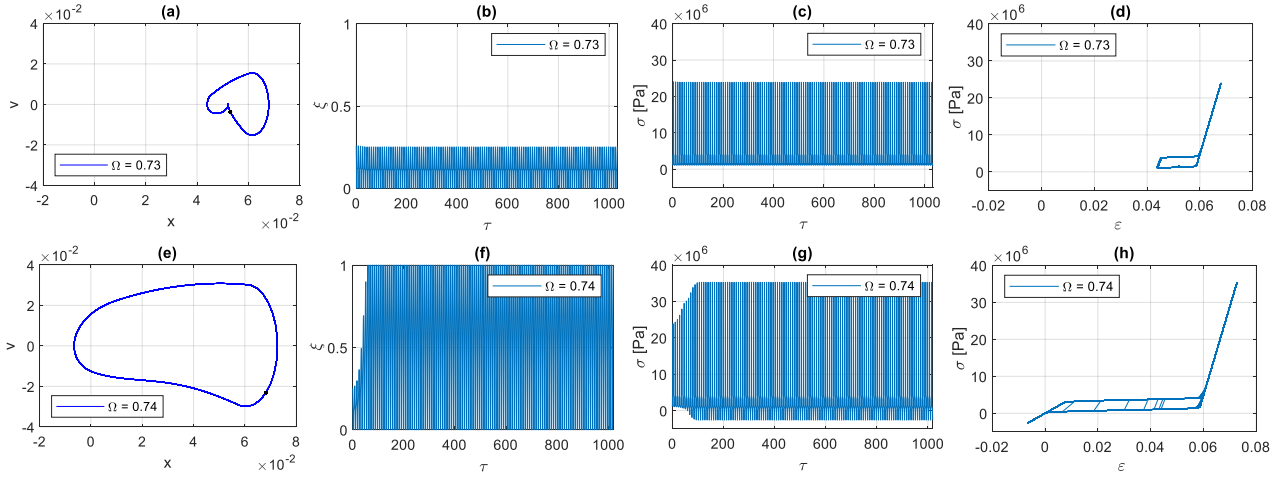

Figure 5 – Responses with magnetic field $\mu_0 H = 0.4$ MA/m: phase-space (a, e); time history of the volume fraction (b, f); time history of the stress (c, g); and stress-strain diagram (d, h) for, respectively, $\Omega = 0.73$ and $\Omega = 0.74$.

The same behavior is observed when the magnetic field is 0.6 MA/m, and the abrupt change in the mean displacement occurs between $\Omega = 0.63$ and $\Omega = 0.64$. Figure 6 shows that the increase of the excitation frequency promotes a more intense reorientation, leading to sudden changes in the mean displacement of the system.

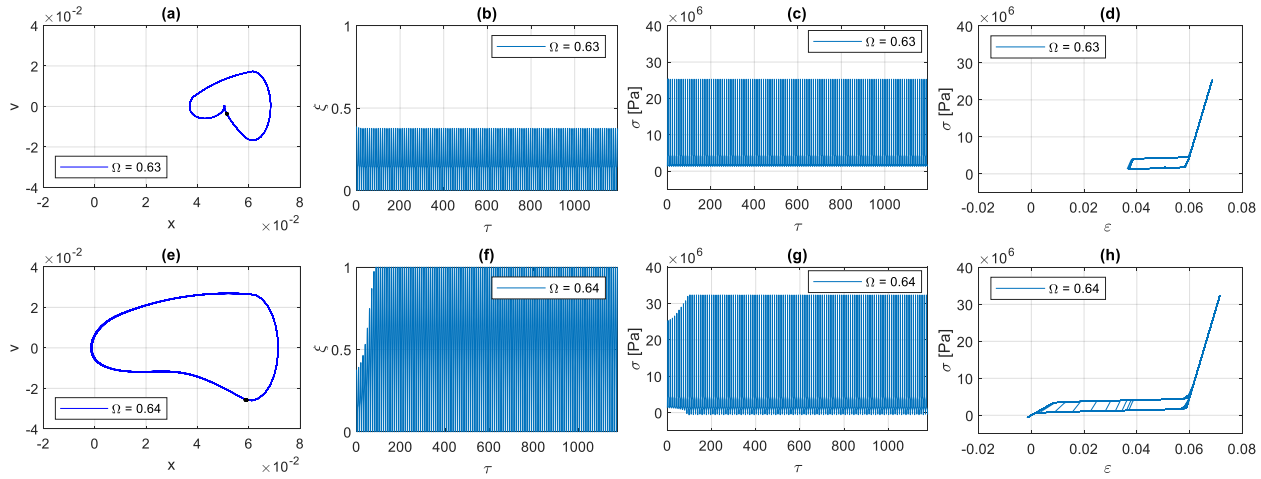

Figure 6 – Responses with magnetic field $\mu_0 H = 0.6$ MA/m : phase-space (a, e); time history of the volume fraction (b, f); time history of the stress (c, g); and stress-strain diagram (d, h) for, respectively, $\Omega = 0.63$ and $\Omega = 0.64$.

A bifurcation diagram is now analyzed by considering the variation of the bias magnetic field, Figure 7, assuming a constant frequency $\Omega = 1.25$. Note that, for lower values of the bias magnetic field, the system shows a period-1 response. As the magnetic field is increased, the system response becomes more complex. The system shifts from a period-1 response to a period-2, then to a period-4 just by increasing the bias magnetic field, reaching a chaotic-like behavior. The system response changes until the critical magnetic field is reached.

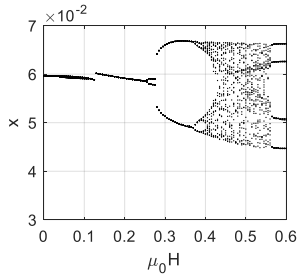

Figure 7 – Bifurcation diagram in respect with $\mu_0 H$.

Figure 8 shows simulation, related to Fig.7, for three bias magnetic field (0.18 MA/m, 0.28 MA/m and 0.38 MA/m), while the excitation frequency is constant at $\Omega = 1.25$ and the stress amplitude is at 5 MPa. Phase-space, time history of the volume fraction and the stress, and stress-strain diagrams of the MSMA element are presented. The martensitic reorientation process during the dynamical response can be observed through the stress-strain diagram and the volume fraction time series. Note that the system presents a period-1 response when the applied field is 0.18 MA/m, changing to a period-2 when it's 0.28 MA/m, and period-4 when it's 0.38 MA/m. Furthermore, the oscillation amplitude seemed to get bigger for higher bias magnetic field values.

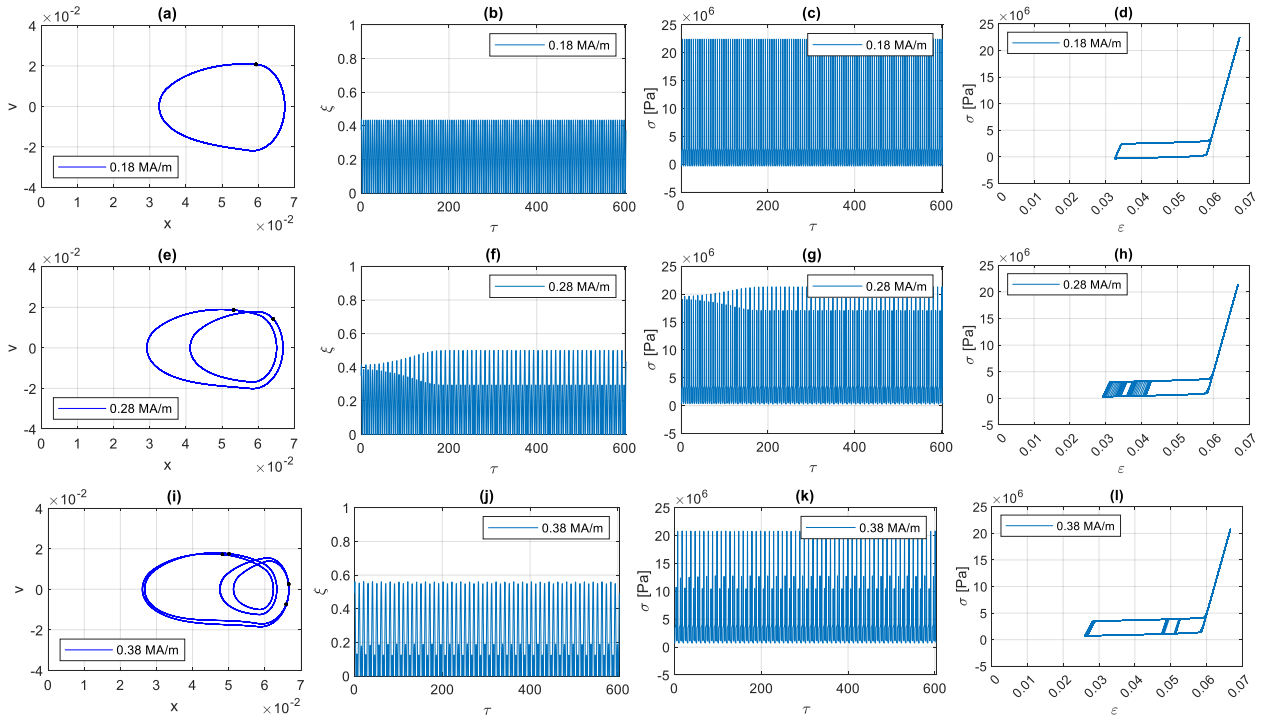

Figure 8 – $\Omega = 1.25$ and $\sigma_0 = 5$ MPa: phase-space (a, e, i); time history of the volume fraction (b, f, j); time history of the stress (c, g, k); and stress-strain diagram (d, h, l) for, respectively, 0.18 MA/m, 0.28 MA/m and 0.38 MA/m.

The root-mean-square displacement of the system for the magnetic field sweep is presented in Fig.9, showing a small reduction at 0.125 MA/m, and after that, x_{rms} remains almost constant for further increase of the magnetic field. These results are better understood by observing the response for 0.125 MA/m and 0.130 MA/m. Figure 10 presents the phase-space, the time history of the volume fraction and the stress, and the stress-strain diagrams of the MSMA rod for these two magnetic field levels. Note that the slight increase in the magnetic field is enough to trigger a more intense variant reorientation, leading to sudden changes in the mean displacement of the system. A similar result of that obtained when the frequency is changed.

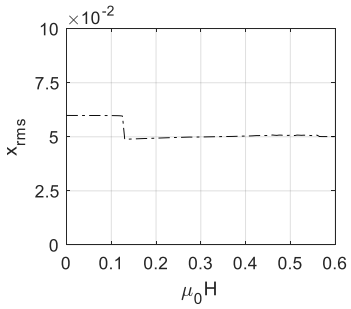

Figure 9 – Root-mean-square position of the system in respect with $\mu_0 H$.

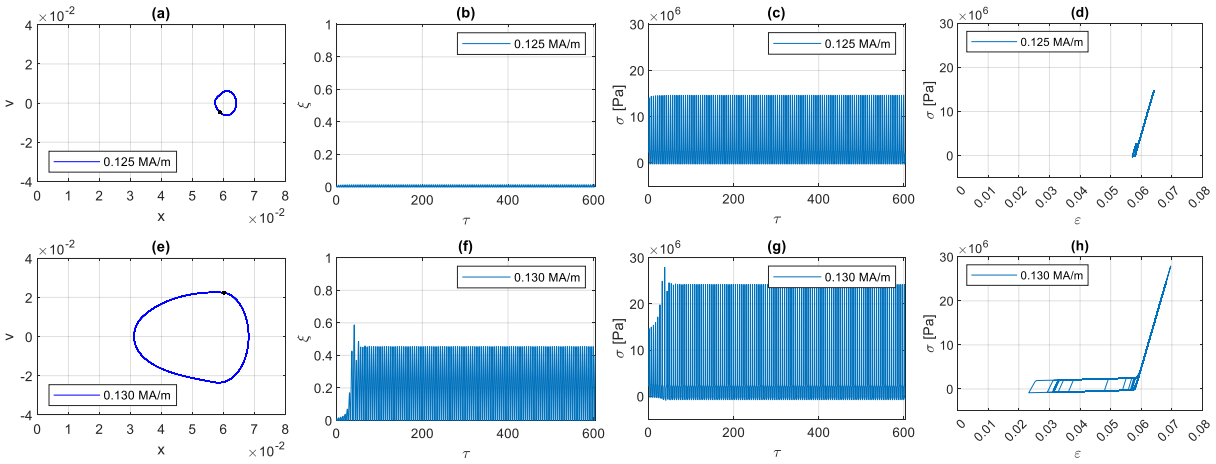

Figure 10 – Responses for $\Omega = 1.25$ and $\sigma_0 = 5$ MPa: phase-space (a, e); time history of the volume fraction (b, f); time history of the stress (c, g); and stress-strain diagram (d, h) for, respectively, 0.125 MA/m and 0.130 MA/m.

Conclusions

This work investigates the nonlinear dynamics of an MSMA system considering a well-established phenomenological model for martensitic reorientation. The operator split technique is employed for numerical simulations. The system behavior is simulated for different magnetic field levels and excitation frequencies. The application of a magnetic field can lead to deep dynamical behavior changes, such as modifying the period of oscillation, and even achieving chaotic-like responses. Just by increasing the excitation frequency or the magnetic field, it is possible to induce changes in the mean displacement of the system due to a more intense variant reorientation. At specific points, abrupt modifications on those parameters are witnessed, followed by smoother variations as the frequency or magnetic field are increased. These possibilities point to potential applications of MSMAs in industrial devices such as active vibration control.

ACKNOWLEDGMENTS

The authors would like to acknowledge the support of the Brazilian agencies CNPq, CAPES and FAPERJ.

REFERENCES

Chen, Xue, and Yongjun He, 2020, “Thermo-Magneto-Mechanical Coupling Dynamics of Magnetic Shape Memory Alloys”, International Journal of Plasticity.

Chen, Xue, Ziad Moumni, Yongjun He, and Weihong Zhang, 2014, “A Three-Dimensional Model of Magneto-Mechanical Behaviors of Martensite Reorientation in Ferromagnetic Shape Memory Alloys”, Journal of the Mechanics and Physics of Solids.

Haldar, Krishnendu, Dimitris C. Lagoudas, and Ibrahim Karaman, 2014, “Magnetic Field-Induced Martensitic Phase Transformation in Magnetic Shape Memory Alloys: Modeling and Experiments”, Journal of the Mechanics and Physics of Solids, Vol.69, pp. 33–66.

Kiefer, B., and D. C. Lagoudas, 2005, “Magnetic Field-Induced Martensitic Variant Reorientation in Magnetic Shape Memory Alloys”, Philosophical Magazine, vol.85, pp. 33–35.

Kiefer, Bjoern, 2007, “A Phenomenological Constitutive Model for Magnetic Shape Memory Alloys”, Texas A&M University.

O’Handley, R. C., 1998, “Model for Strain and Magnetization in Magnetic Shape-Memory Alloys”, Journal of Applied Physics, vol.83.

Shirani, M, and M. Kadkhodaei, 2014b, “A Geometrical Approach to Determine Reorientation Start and Continuation Conditions in Ferromagnetic Shape Memory Alloys Considering the Effects of Loading History”, Smart Materials and Structures, vol.23.

Shirani, Milad, and Mahmoud Kadkhodaei, 2014a, “A Modified Constitutive Model with an Enhanced Phase Diagram for Ferromagnetic Shape Memory Alloys”, Journal of Intelligent Material Systems and Structures, vol.26, pp. 56-68.

Smith, Aaron R., Juhani Tellinen, and Kari Ullakko, 2014, “Rapid Actuation and Response of Ni–Mn–Ga to Magnetic-Field-Induced Stress”, Acta Materialia, vol.80, pp. 373–379.

de Souza, Vandré F., Marcelo A. Savi, Luciana L. Silva Monteiro, and Alberto Paiva, 2018, “Phenomenological Modeling of the Thermo-Magneto-Mechanical Behavior of Magnetic Shape Memory Alloys”, Journal of Intelligent Material Systems and Structures, vol.29, pp. 3696–3709.

Ullakko, K., J. K. Huang, C. Kantner, R. C. O’Handley, and V. V. Kokorin, 1996, “Large Magnetic-field-induced Strains in Ni 2 MnGa Single Crystals”, Applied Physics Letters, vol.69.

Wang, Jiong, and Paul Steinmann, 2012, "A Variational Approach towards the Modeling of Magnetic Field-Induced Strains in Magnetic Shape Memory Alloys", Journal of the Mechanics and Physics of Solids, vol.60, pp. 1179–1200.

RESPONSIBILITY NOTICE

The authors are the only responsible for the printed material included in this paper.